Constraints on Protein Structure in HIV-1 Rev and Rev−RNA Supramolecular Assemblies from Two-Dimensional Solid State Nuclear Magnetic Resonance†

Robert H. Havlin,‡ Francisco J. Blanco,§ and Robert Tycko*,‡

Laboratory of Chemical Physics, National Institute of Diabetes and Digestive and Kidney Diseases, National Institutes of Health, Bethesda, Maryland 20892-0520, and NMR Group, Centro Nacional de Investigaciones Oncológicas, Melchor Fernández Almagro, 3, E-28029 Madrid, Spain

Received November 6, 2006; Revised Manuscript Received January 16, 2007

ABSTRACT: The HIV-1 Rev protein is required for export of partially spliced and unspliced viral mRNA from nuclei of infected cells, and ultimately for viral replication. Rev is highly prone to aggregation, both in the absence and in the presence of the Rev responsive element (RRE) RNA to which it binds. As a result, the full molecular structures of Rev and Rev−RRE complexes are not known. We describe the results of transmission electron microscopy, atomic force microscopy, and solid state nuclear magnetic resonance (NMR) experiments on pure Rev filaments and coassemblies of Rev with a 45-base RNA sequence representing the high-affinity stem−loop IIB segment of the RRE. The morphologies of Rev filaments and Rev−RNA coassemblies are qualitatively different. Nonetheless, two-dimensional (2D) solid state $^{13}C-^{13}C$ NMR spectra of Rev filament and Rev−RNA coassembly samples, in which all Ile, Val, and Ala residues are uniformly labeled with ^{13}C, are nearly indistinguishable, indicating that the protein conformation is essentially the same in the two types of supramolecular assemblies. Analysis of cross-peak patterns in the 2D spectra supports a previously developed helix−loop−helix structural model for the N-terminal half of Rev and shows that this model applies to both Rev filaments and Rev−RNA coassemblies. In addition, the 2D spectra suggest the presence of additional helix content at Ile and Val sites in the C-terminal half of Rev.

Rev is a 116-residue protein encoded by the genome of HIV-1[1] and expressed in infected cells. Rev has been shown (*1*, *2*) to target partially spliced and unspliced viral mRNA for transport from infected cell nuclei to the cytoplasm (where partially spliced mRNA can be translated into the Vif, Vpr, Vpu, and envelope proteins and where unspliced mRNA can be translated into the Gag and Gag-Pol polyproteins or packaged into new virions) by binding to an mRNA segment in the *env* gene known as the Rev responsive element (RRE). The highest-affinity interaction between Rev and the RRE, with a dissociation constant on the order of 1 nM under in vitro conditions, involves the arginine-rich motif (ARM) of Rev, comprised of residues 35−50, and the stem−loop IIB segment of the RRE (*3*−*6*). The nuclear export signal (NES) of Rev, contained in residues 73−83, has been shown to interact with Crm1/exportin 1 and other cellular cofactors (*2*, *7*, *8*), leading to export of Rev−RNA complexes from the nucleus. The nuclear localization signal (NLS) of Rev is contained in the ARM. Dissociation of RNA from Rev in the cytoplasm is believed to expose the NLS, leading to binding to importin-β, transport into the nucleus, and successive rounds of RNA binding and export (*2*, *9*, *10*).

The full molecular structure of Rev is currently unknown, largely because full-length Rev is strongly prone to aggregation in vitro at concentrations above 1 μM, both in the presence and in the absence of RNA (*11*−*14*). Rev assemblies have a highly ordered, filamentous morphology that has been characterized previously by electron microscopy (*12*−*14*). On the basis of circular dichroism (CD) spectroscopy of full-length Rev and Rev fragments, Auer et al. proposed a structural model for Rev monomers in which the N-terminal half of Rev contains two α-helical segments (*15*). One of these, residues 34−59, contains the ARM. Formation of a helix by peptides derived from the Rev ARM has been characterized by CD (*16*) and solution NMR (*17*−*20*). The other α-helical segment was proposed to comprise residues 8−26. Several models for contacts between the two α-helical segments in monomeric Rev have been proposed, based on functional analysis of Rev mutants and protein footprinting (*21*, *22*). Little structural data on the C-terminal half of Rev are available, except for evidence from CD measurements (*15*, *23*) that the C-terminal half is not predominantly helical. A low-resolution structural model for Rev filaments has been

† Supported by the Intramural Research Program of the National Institute of Diabetes and Digestive and Kidney Diseases, a grant to R.T. from the Intramural AIDS Targeted Antiviral Program of the National Institutes of Health, Grant BIO2003-02246 from the Spanish Ministry of Education and Science to F.J.B., and a Ramón y Cajal contract to F.J.B.

* To whom correspondence should be addressed: National Institutes of Health, Building 5, Room 112, Bethesda, MD 20892-05202. Phone: (301)402-8272. Fax: (301)496-0825. E-mail: robertty@mail.nih.gov.

‡ National Institutes of Health.

§ Centro Nacional de Investigaciones Oncológicas.

[1] Abbreviations: HIV-1, human immunodeficiency virus type 1; RRE, Rev responsive element; NMR, nuclear magnetic resonance; 2D, two-dimensional; ARM, arginine-rich motif; NES, nuclear export signal; NLS, nuclear localization signal; CD, circular dichroism; EDTA, ethylenediaminetetraacetic acid; MAS, magic-angle spinning; TEM, transmission electron microscope; AFM, atomic force microscope.

10.1021/bi0622928 CCC: $37.00
Published on Web 02/21/2007

developed by Watts et al., based on cryoelectron microscopy and other measurements (*14*).

The stem−loop IIB segment of the RRE contains a purine-rich bubble whose structure has been determined by solution nuclear magnetic resonance (NMR), both as a free RNA oligomer (*24*, *25*) and as a complex with ARM peptides (*17*, *18*, *25*−*27*), and by crystallography (*28*). Lower-affinity binding sites in the RRE have also been characterized (*3*, *6*, *29*). The full-length RRE is capable of binding approximately eight Rev molecules (*3*), and multimerization of Rev is essential for its biological activity (*30*, *31*). At sufficiently high Rev concentrations, RRE RNA is packaged into ribonucleoprotein complexes that may have a filamentous appearance (*12*, *13*), although with a lower degree of structural order at the resolution of electron microscopy.

In earlier solid state NMR measurements, we used quantitative techniques for constraining protein backbone torsion angles to provide direct evidence for the two α-helical segments in the N-terminal half of Rev in its filamentous form (*23*). These measurements were carried out on Rev filaments in frozen aqueous solution, using protein samples that were expressed with ^{13}C labeling of backbone carbonyl sites in specific amino acid types. CD measurements demonstrated that the helix contents of filamentous and monomeric forms of Rev are indistinguishable (*23*). These earlier solid state NMR measurements represent the only previously published high-resolution, site-specific structural constraints on full-length Rev. The solid state NMR data also suggested that the leucine-rich NES does not adopt a fully extended conformation in Rev filaments and may be partly helical (*23*). Additional direct structural information about the conformation of the C-terminal half of Rev has been lacking.

In this paper, we present new solid state NMR data on Rev, both in pure Rev filaments and in coassemblies with a 45-base RNA that represents the stem−loop IIB segment of the RRE. These data were obtained from samples in which Rev was labeled with ^{13}C at all carbon sites in all Ala, Val, and Ile residues. Each of these residue types occurs five times in the Rev sequence and is present in both the N-terminal half and the C-terminal half. Two-dimensional (2D) ^{13}C−^{13}C NMR spectroscopy allows signals from Ala, Val, and Ile residues to be resolved from one another. Analysis of the 2D NMR cross-peak line shapes permits us to estimate the numbers of each residue type that participate in helical secondary structure, providing evidence of partial helical secondary structure in the C-terminal half of Rev in addition to the N-terminal helical structure identified in earlier measurements. The new solid state NMR data also permit a direct comparison of protein structures in the pure Rev filaments and in the Rev−RNA coassemblies. Importantly, the solid state NMR spectra of the two forms are nearly indistinguishable, demonstrating that binding to RNA does not involve a major protein structural change.

MATERIALS AND METHODS

Protein Expression, Purification, and Filament Formation. HIV-1 Rev (sequence, MAGRSGDSDEDLLKAVRLIKFL-YQSNPPPNPEGTRQARRNRRRRWRERQRQIHSISERI-LSTYLGRSAEPVPLQLPPLERLTLDCNEDCGTSGTQ-GVGSPQILVESPTVLESGAKE, corresponding to the BH10 isolate of HIV-1) was expressed in BL21(DE3) *Escherichia coli* cells using an optimized, synthetic gene in plasmid pET11d. Culture growth conditions, growth media, and Rev purification conditions were as previously described (*23*). The expression medium contained uniformly ^{15}N- and ^{13}C-labeled L-alanine, L-isoleucine, and L-valine and unlabeled versions of all other amino acids. Rev filaments were formed by gradual ultrafiltration of a 1.5 μM solution at 4 °C as previously described (*23*), using membranes with a 3 kDa cutoff and reaching a final Rev concentration of approximately 100 μM over a period of several days. For solid state NMR, Rev filaments were pelleted and resuspended in ultrafiltration buffer [50 mM sodium phosphate, 150 mM NaCl, 50 mM sodium citrate, 1 mM dithiothreitol, and 1 mM ethylenediaminetetraacetic acid (EDTA) (pH 7.0)], producing a Rev concentration of approximately 3 mM in a 235 μL sample volume. $CuNa_2EDTA$ was added to solid state NMR samples at a final concentration of 20 mM to reduce proton spin−lattice relaxation times to approximately 1 s, allowing NMR data acquisition on frozen solutions in a reasonable time frame (*23*, *32*, *33*). NMR samples were frozen in 6 mm diameter magic-angle spinning (MAS) rotors by immersion in liquid nitrogen and were stored at −80 °C.

Rev−RNA coassemblies were formed by ultrafiltration of a solution of purified, isotopically labeled Rev and synthetic RNA (CureVac GmbH, Tübingen, Germany). The RNA sequence was GCU GGU AUG GGC GCA GCG UCA AUG ACG CUG ACG GUA CAG GCC AGC, representing the stem−loop IIB segment of the RRE. This RNA sequence is essentially the same as the sequence used in earlier studies of the binding of Rev ARM peptides to the stem−loop IIB segment (*5*, *16*, *34*) and has been shown to bind Rev ARM peptides with dissociation constants of approximately 30 nM (*16*, *34*). Similar RNA sequences bind full-length Rev with dissociation constants of approximately 3 nm (*12*). Rev and RNA concentrations at the beginning of ultrafiltration were 2.0 μM. Conditions for ultrafiltration and subsequent treatment were identical to those for pure Rev filaments, except that NaCl was omitted from the ultrafiltration buffer.

Frozen solutions were used for solid state NMR measurements, rather than lyophilized samples, to avoid the possibility that lyophilization might perturb the Rev and Rev−RNA structures.

Electron Microscopy and Atomic Force Microscopy. Transmission electron microscope (TEM) images were obtained with an FEI Morgagni microscope, operating at 80 kV. TEM grids were 300 mesh copper grids covered with lacey carbon (Electron Microscopy Sciences), upon which evaporated carbon films (5−10 nm thickness) were deposited. Grids were freshly glow-discharged in air at approximately 250 mTorr. Pelleted Rev and Rev−RNA samples, as used for solid state NMR measurements, were diluted by a factor of 10 in deionized H_2O immediately before adsorption to the carbon films on the TEM grids. One 10 μL aliquot of Rev or Rev−RNA complex was placed on a grid for 2 min, blotted, immediately rinsed once with 10 μL of deionized H_2O, blotted again, immediately stained with 10 μL of 1% (w/v) uranyl acetate, blotted again, and dried in air.

Atomic force microscope (AFM) images were obtained in air with a MultiMode AFM system (Veeco Instruments) in tapping mode, using micro-actuated silicon probes (Veeco

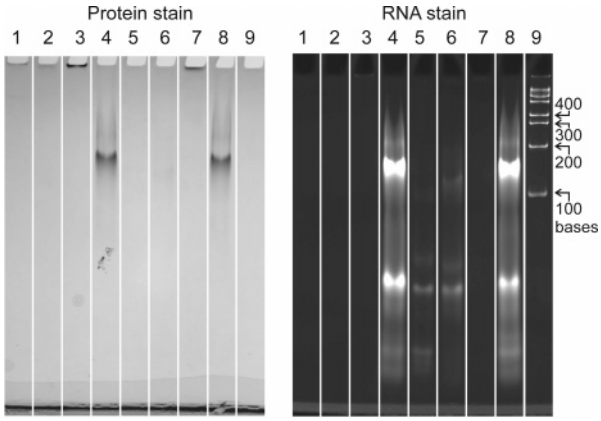

FIGURE 1: Characterization of Rev (lanes 1−3 and 7) and Rev−RNA (lanes 4−6 and 8) samples by gel electrophoresis (10% polyacrylamide, Tris/borate/EDTA running buffer, 150 V applied potential, 30 min run time). The gel was stained for protein with Coomassie Blue (visualized at the left) and for RNA with ethidium bromide (visualized at the right). Rev and Rev−RNA assemblies, prepared for solid state NMR and other measurements, were diluted by a factor of 10 in pure H_2O (or 8 M urea) and combined with an equal volume of 2× RNA loading dye solution (Fermentas) before being loaded on the gel: (1) total Rev filament solution, (2) Rev pellet after centrifugation, (3) Rev supernatant, (4) Rev−RNA pellet after centrifugation, (5) Rev−RNA supernatant, (6) supernatant after washing of the Rev−RNA pellet, (7) Rev pellet, treated with urea before loading, (8) Rev−RNA pellet, treated with urea before loading, and (9) RNA molecular weight markers (Fermentas RiboRuler, low range).

Instruments) with a nominal tip radius of 10 nm and a nominal force constant of 1 N/m. Pelleted Rev and Rev−RNA samples were diluted by a factor of 10 in either deionized H_2O or 0.3% acetic acid (producing pH 3) immediately before adsorption to freshly cleaved mica. One 50 μL aliquot was placed on a 1 cm^2 mica surface for 2 min, blotted, and dried under a stream of nitrogen gas. Approximately 100 images with 5 μm × 5 μm or 10 μm × 10 μm areas were recorded for each AFM sample to ensure that the reported features are truly representative.

Solid State NMR. Solid state NMR measurements were performed at 9.39 T (400.9 MHz ^{1}H NMR frequency; 100.8 MHz ^{13}C NMR frequency) using a Varian Infinity spectrometer and a Varian 6 mm MAS NMR probe. The NMR probe was precooled before samples were introduced, so Rev and Rev−RNA samples remained below −80 °C after initial freezing until solid state NMR measurements were completed. Measurements themselves were performed at −120 °C. At this temperature, we expect protein motions to be largely quenched, allowing ^{13}C NMR signal intensities to be analyzed without consideration of motional effects (e.g., transverse spin relaxation, motional averaging of dipole−dipole couplings).

Two-dimensional solid state ^{13}C−^{13}C NMR spectra were recorded at a MAS frequency of 6.70 kHz, using ramped-amplitude cross polarization (*35*−*37*), two-pulse phase-modulated proton decoupling (*38*) with an 80 kHz decoupling field, and radio frequency-driven recoupling (*39*, *40*) of ^{13}C nuclei for 1.79 ms between the t_1 and t_2 spectral dimensions. The 2D spectrum of the Rev sample was obtained with a 50 μs t_1 increment, 128 complex t_1 points, and 48 scans per free induction decay. The 2D spectrum of the Rev−RNA sample was obtained with a 30 μs t_1 increment, 128 complex t_1 points, and 384 scans per free induction decay. ^{13}C NMR chemical shifts are reported relative to tetramethylsilane, based on an external adamantane methylene carbon reference at 38.56 ppm.

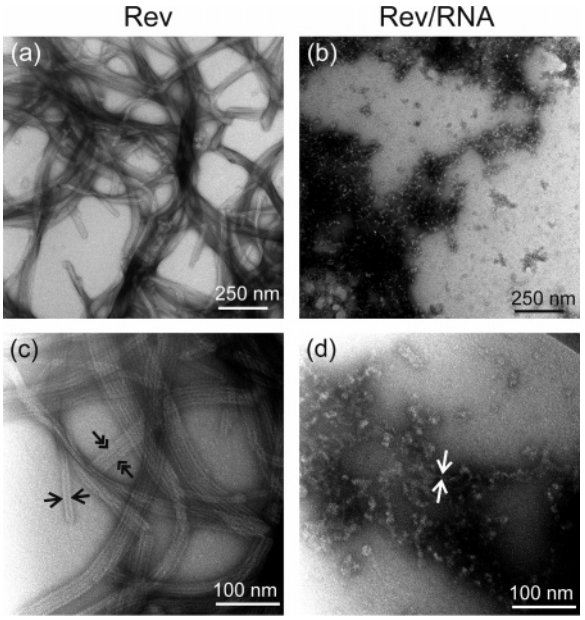

FIGURE 2: Representative TEM images of Rev filaments (a and c) and Rev−RNA coassemblies (b and d), negatively stained with uranyl acetate. Single and double arrowheads in panel c indicate the widths of single and paired Rev filaments, respectively. Single arrowheads in panel d indicate the approximate width of a Rev−RNA coassembly.

RESULTS

Gel Electrophoresis and Microscopy Distinguish Rev Filaments and Rev−RNA Coassemblies. Figure 1 shows the results of gel electrophoresis measurements on Rev filaments and Rev−RNA coassemblies. The electric field in these measurements is directed upward, causing negatively charged molecules or complexes to move downward into the gel. None of the Rev filament preparations (lanes 1−3 and 7) migrate into the gel, as the Rev protein alone is positively charged. The Rev−RNA pellet (lane 4) exhibits a strong band that stains for both protein and RNA, as well as a more rapidly migrating band that stains for only RNA. Addition of 8 M urea (lane 8) does not affect these bands. The supernatant of the pelleted Rev−RNA sample (lane 5) exhibits only a weak, rapidly migrating band that can be attributed to unbound RNA. These electrophoresis results demonstrate that the Rev−RNA coassemblies contain both biopolymers together in a bound state with an overall negative charge, capable of carrying the protein into the gel and not dissociated by urea treatment. A fraction of the RNA in the pelleted Rev−RNA sample migrates in a manner independent of the protein, but most of the RNA remains bound under the conditions of these measurements. This result is consistent with the approximate 1.5:1.0 stoichiometry. Relatively little RNA does not pellet with the Rev−RNA coassemblies.

Figure 2 shows TEM images of Rev filaments and Rev−RNA coassemblies prepared as described above. In agreement with previous studies (*12*−*14*), the Rev filaments (Figure 2a,c) are highly ordered and straight over 100 nm length scales. In these negatively stained images, the Rev

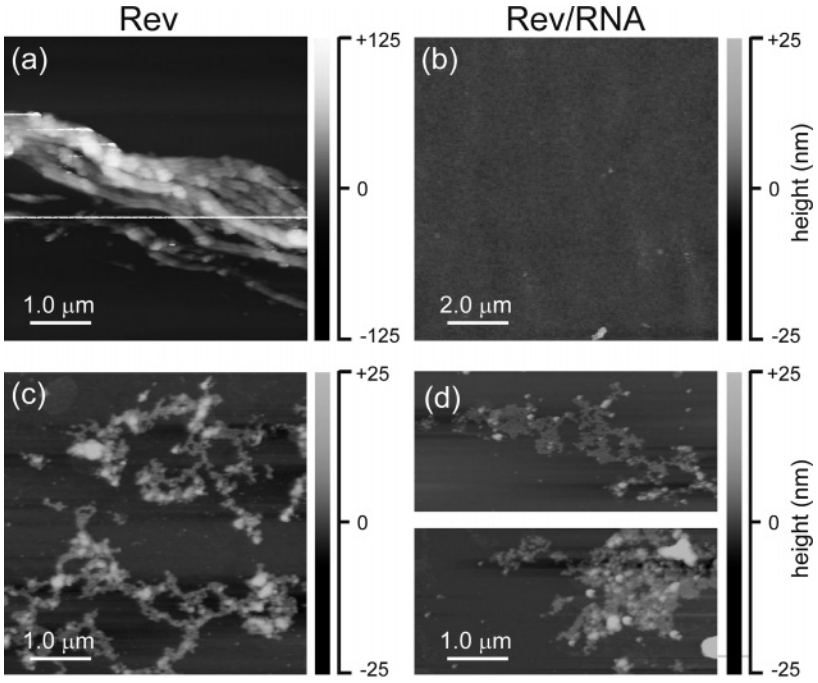

FIGURE 3: Representative AFM images of Rev filaments (a and c) and Rev−RNA coassemblies (b and d), deposited on mica from pH 7 (a and b) and pH 3 (c and d) solutions. The gray scale indicates height above the mica surface.

filaments appear as parallel bundles of light bands, spaced 6 ± 1 nm apart. Although it is tempting to infer from these images that each Rev filament has a diameter of 6 ± 1 nm, earlier studies (*12*−*14*) reached the conclusion that Rev filaments are in fact hollow tubes with diameters of approximately 12 nm and that these tubes are readily filled with uranyl acetate stain, accounting for the regular 6 nm spacing of the light bands when Rev filaments form laterally associated bundles. This interpretation of negatively stained TEM images is supported by the observation that the light bands occur almost exclusively in even numbers in our images. Also in agreement with previous studies (*12*, *13*), Rev−RNA coassemblies (Figure 2b,d) are less well ordered and are approximately 7 ± 2 nm in diameter. The Rev−RNA coassemblies in Figure 2 are approximately 15−30 nm in length. We avoid the term "cofilaments" to describe Rev−RNA coassemblies, as their filamentous nature is not clear from the images in Figure 2. Differences between the Rev−RNA morphologies in Figure 2 and filamentous Rev−RNA morphologies reported in earlier work may be due to significant differences in fibril formation protocols, in RNA sequence, and in stoichiometry.

Figure 3 shows topographic AFM images of the same Rev and Rev−RNA samples, deposited on mica from pH 7 (Figure 3a,b) and pH 3 (Figure 3c,d) solutions. At pH 7, Rev filaments are visible, with minimum heights of 22 ± 3 nm that may represent twice the diameter of a single filament and widths of approximately 130 nm that presumably represent the widths of laterally associated filament bundles (broadened by approximately 10 nm due to the non-negligible radius of curvature of the AFM probe tip). No filamentous structures and very few structures of any type were observed in AFM images of the Rev−RNA sample at pH 7, although the sample deposition and image acquisition procedures were identical to those used for Rev filaments. This result can be explained by the fact that an unmodified mica surface is negatively charged (*41*), promoting the adsorption of positively charged Rev filaments but not Rev−RNA coassemblies if their surface is negatively charged. At pH 3, the Rev filaments appear to be significantly more disordered and have heights of 7 ± 1 nm, suggesting that the filament structure is disrupted at low pH. Rev−RNA coassemblies are observed at pH 3, presumably because the surface charge is no longer negative. Although the Rev−RNA coassemblies are similar in appearance to the disordered Rev filaments at pH 3, they are less filamentous in morphology and are smaller in height (ranging from 3 to 6 nm).

The clear differences in TEM and AFM images of Rev and Rev−RNA samples in Figures 2 and 3 provide further evidence that the Rev−RNA coassemblies contain both Rev and RNA and are distinct from Rev filaments. The TEM results are also inconsistent with the possibility that Rev−RNA coassemblies are fully formed Rev filaments with an outer "coating" of RNA, as such a structure would be expected to have a straight, rodlike morphology similar to that of an individual Rev filament.

Solid State NMR Indicates Indistinguishable Protein Secondary Structures in Rev Filaments and Rev−RNA Coassemblies. Figure 4 shows 2D $^{13}C-^{13}C$ solid state NMR spectra of frozen solutions of Rev filaments and Rev−RNA coassemblies. In both samples, all Val, Ala, and Ile residues were uniformly labeled with ^{15}N and ^{13}C. Under the conditions of these measurements (see Materials and Methods), strong cross-peaks that connect the chemical shifts of directly bonded carbon sites in the labeled residues are observed. Residue type assignments of cross-peaks can be obtained from the 2D spectra (Figure 4e,f), but direct site-specific assignments are not possible with the isotopic labeling scheme employed here. The five Ile residues in Rev exhibit a single set of cross-peaks with approximately symmetric, Gaussian shapes, indicating similar protein conformations at the five Ile sites. In contrast, Ala and Val residues exhibit highly asymmetric cross-peaks, indicating conformational variations among the five Ala sites and the

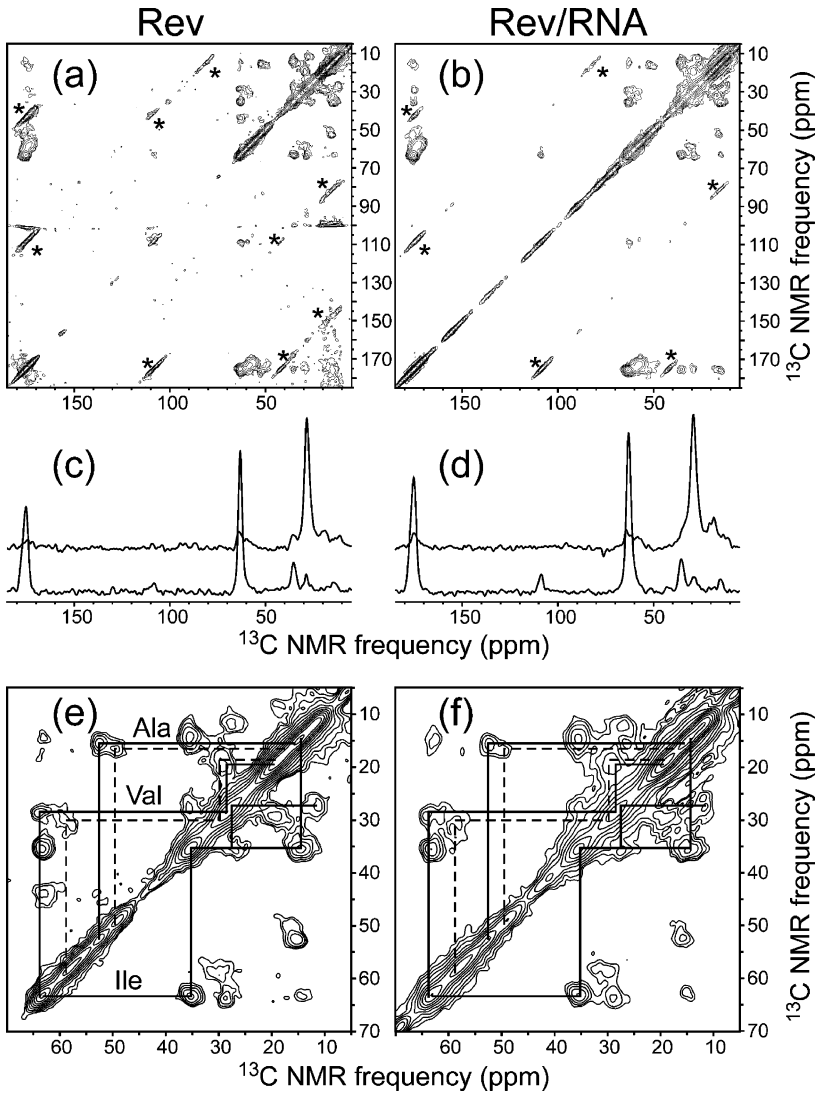

FIGURE 4: 2D $^{13}C-^{13}C$ solid state NMR spectra of Rev filaments (a, c, and e) and Rev−RNA coassemblies (b, d, and f) obtained at 100.8 MHz with magic-angle spinning at 6.7 kHz. The Rev protein is uniformly labeled with ^{15}N and ^{13}C at all Ala, Val, and Ile residues. Spectra were obtained from frozen solutions at −120 °C. (a and b) Full spectra, with asterisks indicating spinning sideband artifacts. (c and d) One-dimensional slices at 63 and 29 ppm, to illustrate the signal-to-noise ratio. (e and f) Expansions of the aliphatic regions. Assignment paths connecting strong one-bond cross-peaks are shown for both helical (—) and nonhelical (- - -) components.

five Val sites. 2D spectra of Rev filaments and Rev−RNA coassemblies are remarkably similar. The greater diagonal signal intensity in the Rev−RNA spectrum, particularly between 70 and 160 ppm, can be attributed to natural-abundance ^{13}C NMR signals from the RNA.

Our protocol for Rev filament production results in morphologically homogeneous samples. Amorphous Rev aggregates constitute a negligible fraction of the NMR samples, as indicated by the TEM images in Figure 2 and by earlier solid state NMR results (*23*). The asymmetry of Ala and Val cross-peaks is therefore due to site-specific conformational variations within each Rev molecule, rather than to structural variation among molecules.

As established by many earlier experimental and computational studies (*42*−*48*), ^{13}C NMR chemical shifts, especially those of C_α and C_β sites, are strongly correlated with protein secondary structure. In helical segments, C_α lines move downfield and C_β lines move upfield relative to "random coil" chemical shifts (i.e., chemical shifts of small peptides in solution that lack persistent secondary structure). We can therefore use the experimental $C_\alpha-C_\beta$ cross-peaks in Figure 4 to place constraints on the secondary structure of Rev at the labeled residues. The $C_\alpha-C_\beta$ cross-peaks of Ile, Ala, and Val residues all exhibit components that can be assigned to helical conformations (see Table 1). The Ala and Val residues also exhibit nonhelical components. To assess the number of helical and nonhelical residues of each type, signal volumes contained within polygonal regions enclosing the helical and nonhelical components were measured, using the regions displayed in Figure 5. The results are given in Table 2. Helical signal fractions for the Rev filaments and the Rev−

Table 1: ^{13}C NMR Chemical Shifts in Rev Filaments, in Parts per Million Relative to Tetramethylsilane[a]

residue type	helical C_α shift	helical C_β shift	nonhelical C_α shift	nonhelical C_β shift
Ile	63.4 (59.4)	35.4 (37.1)	–	–
Ala	52.7 (50.8)	15.2 (17.4)	49.6	16.5
Val	63.9 (60.5)	28.7 (31.2)	58.2	29.8

[a] Nonhelical shifts are the approximate centroids of nonhelical signal regions. Values in parentheses are random coil shifts, taken from ref *50*.

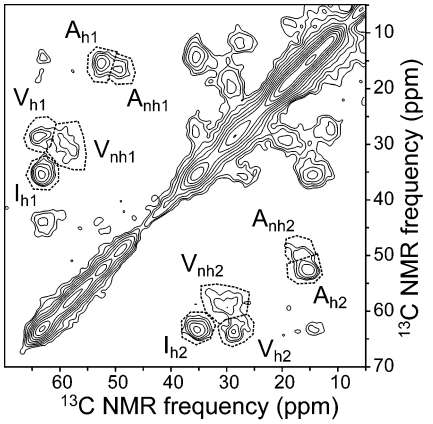

FIGURE 5: Aliphatic region of the 2D $^{13}C-^{13}C$ solid state NMR spectrum of Rev filaments, showing polygonal signal integration regions in dashed lines. Helical and nonhelical signal regions of $C_\alpha-C_\beta$ cross-peaks for residue type X are labeled X_{h1} (or X_{h2}) and X_{nh1} (or X_{nh2}).

RNA coassemblies are indistinguishable. These results are most consistent with five Ile residues, three Ala residues, and two Val residues existing in helical segments, both in Rev filaments and in Rev−RNA coassemblies. The two remaining Ala residues and three Val residues would then be in nonhelical (possibly but not necessarily disordered) segments. Because the solid state NMR measurements were performed at sample temperatures of −120 °C, protein segments that may be flexible and dynamic in a fluid aqueous environment are rigid in these measurements. We therefore expect all residues of a given type to contribute equal signal volumes to the $C_\alpha-C_\beta$ cross-peaks, regardless of their location in the Rev sequence.

The total ^{13}C NMR signal from Ala residues, relative to the total signal from Ile residues, is weaker in the 2D spectrum of the Rev−RNA sample than in the 2D spectrum of the Rev sample by approximately 27%. The total ^{13}C NMR signal from Val residues is stronger by approximately 11%. These variations in total signal intensities may be due to variations in the level of incorporation of isotopically labeled L-alanine and L-valine. In earlier work using the same protein expression protocol (*23*), the levels of incorporation of isotopically labeled L-alanine and L-valine were determined to be 50 ± 15 and >90%, respectively. Sample-to-sample variations in isotopic enrichment are not unexpected, but we expect the level of enrichment to be the same for all residues of a given type in a given sample.

DISCUSSION

The BH10 Rev sequence contains Ile at positions 19, 52, 55, 59, and 102, Ala at positions 2, 15, 37, 68, and 114, and Val at positions 16, 71, 97, 104, and 109. Previous studies (*15*, *21*, *22*), including solid state NMR measurements of Rev filaments by Blanco et al. (*23*), support a helix−turn−helix structural motif for the N-terminal half of Rev in which residues 8−26 and 34−59 form α-helices (although direct NMR evidence for helix−helix tertiary contacts has not yet been obtained). These previously identified helical segments account for four helical Ile residues, two helical Ala residues, and one helical Val residue. The solid state NMR data described above are consistent with these previously identified helical segments and indicate that one additional residue of each type has backbone torsion angles that correspond to a helical conformation. The additional helical Ile residue can only be Ile102. The additional helical Val residue may be Val104, suggesting the possibility that residues 102−104 form part of an α-helical segment. The additional helical Ala residue may be Ala2, suggesting that the first helical segment may begin before Ser8 in Rev filaments and Rev−RNA coassemblies.

Table 2: Analysis of $C_\alpha-C_\beta$ Cross-Peak Volumes in 2D $^{13}C-^{13}C$ Solid state NMR Spectra of Rev Filaments and Rev−RNA Coassemblies[a]

sample	integration region	volumes above and below diagonal (e.g., V_{h1}, V_{h2})	total volume	helical fraction
Rev	V_h	24, 21	45	0.35 ± 0.04
	V_{nh}	36, 48	84	
	A_h	30, 30	60	0.56 ± 0.05
	A_{nh}	25, 23	48	
	I_h	48, 52	100	1.00 ± 0.07
Rev−RNA	V_h	21, 26	47	0.33 ± 0.04
	V_{nh}	51, 45	96	
	A_h	27, 18	45	0.57 ± 0.06
	A_{nh}	18, 16	34	
	I_h	48, 52	100	1.00 ± 0.07

[a] Volumes are normalized to I_h for each sample. Individual volume measurements have uncertainties of approximately ±5 due to noise in the experimental spectra.

Earlier CD measurements indicated that a monomeric Rev deletion mutant, in which residues 68−112 were deleted, has a helix content of 65% (*15*) and that full-length Rev in filamentous form has a helix content of 49% (*23*). These CD results correspond to approximately 46 helical residues in the deletion mutant and approximately 57 helical residues in the full-length, filamentous protein. Raman spectroscopy indicates a helix content of 54% in full-length Rev filaments (*14*). The assignment of additional helical Ile, Val, and Ala residues suggested above is consistent with these CD and Raman results. Additional solid state NMR measurements on samples with different isotopic labeling patterns would be required for the unambiguous determination of these assignments.

Given the pronounced differences in the morphology and dimensions of Rev filaments and Rev−RNA coassemblies in Figures 2 and 3, the similarity of 2D $^{13}C-^{13}C$ solid state NMR spectra of Rev filaments and Rev−RNA coassemblies is surprising. ^{13}C chemical shifts for labeled sites are nearly identical in the two samples, and the helical fractions for Ile, Ala, and Val residues are indistinguishable. These observations strongly suggest that the protein structure is essentially the same in both samples, i.e., that the Rev−RNA interaction does not require a major conformational change in the protein. Although TEM and AFM images indicate that Rev−RNA coassemblies are more disordered than Rev filaments on the 5−10 nm length scale, the solid state NMR spectra show no difference in structural order at the molecular level; i.e., ^{13}C NMR line widths are not significantly larger in spectra of the Rev−RNA coassemblies.

Watts et al. have proposed a low-resolution model for Rev filaments, according to which these filaments are hollow tubes constructed from Rev dimers, arranged in a six-start helical pattern (*14*). In this model, which is based on cryoelectron microscopy of frozen hydrated samples, mea-

surements of mass per length via scanning transmission electron microscopy of the freeze-dried samples, electron diffraction, and Raman spectroscopy, N-terminal helical segments are located on the inner walls of the tubes and are approximately parallel to the long axes of the tubes. Other molecular-level details are not given. We are not aware of any published models for the structure of Rev−RNA coassemblies, other than models for ARM peptide−RNA complexes derived from solution NMR data (*17*, *18*, *27*). If the model of Watts et al. for pure Rev filaments also applied to Rev−RNA coassemblies, then one would expect the RNA to fill the center of the coassembly, where the RRE could interact with the ARM helix. Such a structure might be consistent with the solid state NMR data but would be inconsistent with the dimensions of the Rev−RNA coassemblies observed in our TEM images (Figure 2b,d). Thus, assuming that the model of Watts et al. is at least approximately correct, our data show that Rev assembles into two qualitatively different supramolecular structures without a detectable change in protein conformation. (More subtle changes in protein conformation may become apparent when additional solid state NMR measurements on samples with different isotopic labeling patterns are performed.) In our protocol for formation of Rev−RNA coassemblies, it seems likely that Rev binds to stem−loop IIB RNA before its aggregation into the large supramolecular structures observed in TEM images, rather than first forming large Rev aggregates that subsequently interact with RNA. This mode of Rev−RNA assembly would be consistent with previous observations that Rev−RNA coassemblies form more rapidly and at lower protein concentrations than pure Rev filaments do (*11*, *13*).

The TEM and AFM images in Figures 2 and 3 provide additional, albeit indirect, constraints on the structure of Rev−RNA coassemblies. The TEM images indicate that Rev−RNA coassemblies have a diameter of 7 ± 2 nm, a factor of nearly 2 times narrower than Rev filaments. The AFM measurements, in particular the absence of detectable adsorption of Rev−RNA coassemblies to mica from pH 7 solutions, suggest that the surface of Rev−RNA coassemblies is negatively charged, given the negative charge of the mica surface. A negative surface could be created either by placing the RNA on the exterior of the Rev−RNA coassemblies, which would then have a proteinaceous core with ARM helices directed toward the exterior for interaction with the RNA, or by partially sequestering the RNA and ARM helices in the interior of the coassemblies and exposing the C-terminal half of Rev (with a net charge of −6 from Glu69 through Glu111 at pH 7). The latter possibility may favor exposure of the NES for interaction with Crm1/exportin 1 (*2*, *7*, *8*). The Rev−RNA coassemblies shown in Figure 2 are not too large to pass through a nuclear pore (*49*), suggesting that they are relevant models for coassemblies in infected cells. We note that, although experimental evidence cited above supports the formation of Rev−RNA coassemblies in vivo, no evidence of pure Rev filament formation in vivo exists currently.

ACKNOWLEDGMENT

We thank Dr. Simon Sharpe for assistance with electrophoresis experiments and Javier Pérez Altozano for help with the purification of Rev.

REFERENCES

1. Cullen, B. R. (1998) Posttranscriptional regulation by the HIV-1 Rev protein, *Semin. Virol. 8*, 327−334.
2. Pollard, V. W., and Malim, M. H. (1998) The HIV-1 Rev protein, *Annu. Rev. Microbiol. 52*, 491−532.
3. Daly, T. J., Doten, R. C., Rennert, P., Auer, M., Jaksche, H., Donner, A., Fisk, G., and Rusche, J. R. (1993) Biochemical characterization of binding of multiple HIV-1 Rev monomeric proteins to the Rev responsive element, *Biochemistry 32*, 10497−10505.
4. Heaphy, S., Dingwall, C., Ernberg, I., Gait, M. J., Green, S. M., Karn, J., Lowe, A. D., Singh, M., and Skinner, M. A. (1990) HIV-1 regulator of virion expression (Rev) protein binds to an RNA stem-loop structure located within the Rev response element region, *Cell 60*, 685−693.
5. Kjems, J., Calnan, B. J., Frankel, A. D., and Sharp, P. A. (1992) Specific binding of a basic peptide from HIV-1 Rev, *EMBO J. 11*, 1119−1129.
6. Van Ryk, D. I., and Venkatesan, S. (1999) Real-time kinetics of HIV-1 Rev-Rev response element interactions: Definition of minimal binding sites on RNA and protein and stoichiometric analysis, *J. Biol. Chem. 274*, 17452−17463.
7. Elfgang, C., Rosorius, O., Hofer, L., Jaksche, H., Hauber, J., and Bevec, D. (1999) Evidence for specific nucleocytoplasmic transport pathways used by leucine-rich nuclear export signals, *Proc. Natl. Acad. Sci. U.S.A. 96*, 6229−6234.
8. Yi, R., Bogerd, H. P., and Cullen, B. R. (2002) Recruitment of the Crm1 nuclear export factor is sufficient to induce cytoplasmic expression of incompletely spliced human immunodeficiency virus mRNAs, *J. Virol. 76*, 2036−2042.
9. Henderson, B. R., and Percipalle, P. (1997) Interactions between HIV Rev and nuclear import and export factors: The Rev nuclear localisation signal mediates specific binding to human importin-*β*, *J. Mol. Biol. 274*, 693−707.
10. Fineberg, K., Fineberg, T., Graessmann, A., Luedtke, N. W., Tor, Y., Rui, L. X., Jans, D. A., and Loyter, A. (2003) Inhibition of nuclear import mediated by the Rev arginine-rich motif by RNA molecules, *Biochemistry 42*, 2625−2633.
11. Cole, J. L., Gehman, J. D., Shafer, J. A., and Kuo, L. C. (1993) Solution oligomerization of the Rev protein of HIV-1: Implications for function, *Biochemistry 32*, 11769−11775.
12. Heaphy, S., Finch, J. T., Gait, M. J., Karn, J., and Singh, M. (1991) Human immunodeficiency virus type 1 regulator of virion expression, Rev, forms nucleoprotein filaments after binding to a purine-rich bubble located within the Rev responsive region of viral messenger RNAs, *Proc. Natl. Acad. Sci. U.S.A. 88*, 7366−7370.
13. Wingfield, P. T., Stahl, S. J., Payton, M. A., Venkatesan, S., Misra, M., and Steven, A. C. (1991) HIV-1 Rev expressed in recombinant *Escherichia coli*: Purification, polymerization, and conformational properties, *Biochemistry 30*, 7527−7534.
14. Watts, N. R., Misra, M., Wingfield, P. T., Stahl, S. J., Cheng, N. Q., Trus, B. L., Steven, A. C., and Williams, R. W. (1998) Three-dimensional structure of HIV-1 Rev protein filaments, *J. Struct. Biol. 121*, 41−52.
15. Auer, M., Gremlich, H. U., Seifert, J. M., Daly, T. J., Parslow, T. G., Casari, G., and Gstach, H. (1994) Helix-loop-helix motif in HIV-1 Rev, *Biochemistry 33*, 2988−2996.
16. Tan, R. Y., Chen, L., Buettner, J. A., Hudson, D., and Frankel, A. D. (1993) RNA recognition by an isolated α-helix, *Cell 73*, 1031−1040.
17. Battiste, J. L., Mao, H. Y., Rao, N. S., Tan, R. Y., Muhandiram, D. R., Kay, L. E., Frankel, A. D., and Williamson, J. R. (1996) α-Helix-RNA major groove recognition in an HIV-1 Rev peptide RRE RNA complex, *Science 273*, 1547−1551.
18. Peterson, R. D., and Feigon, J. (1996) Structural change in Rev responsive element RNA of HIV-1 on binding Rev peptide, *J. Mol. Biol. 264*, 863−877.
19. Scanlon, M. J., Fairlie, D. P., Craik, D. J., Englebretsen, D. R., and West, M. L. (1995) NMR solution structure of the RNA-binding peptide from human immunodeficiency virus type 1 Rev, *Biochemistry 34*, 8242−8249.
20. Ye, X. M., Gorin, A., Ellington, A. D., and Patel, D. J. (1996) Deep penetration of an α-helix into a widened RNA major groove in the HIV-1 Rev peptide-RNA aptamer complex, *Nat. Struct. Biol. 3*, 1026−1033.

21. Thomas, S. L., Hauber, J., and Casari, G. (1997) Probing the structure of the HIV-1 Rev transactivator protein by functional analysis, *Protein Eng. 10*, 103−107.
22. Jensen, T. H., Jensen, A., Szilvay, A. M., and Kjems, J. (1997) Probing the structure of HIV-1 Rev by protein footprinting of multiple monoclonal antibody-binding sites, *FEBS Lett. 414*, 50−54.
23. Blanco, F. J., Hess, S., Pannell, L. K., Rizzo, N. W., and Tycko, R. (2001) Solid state NMR data support a helix-loop-helix structural model for the N-terminal half of HIV-1 Rev in fibrillar form, *J. Mol. Biol. 313*, 845−859.
24. Peterson, R. D., Bartel, D. P., Szostak, J. W., Horvath, S. J., and Feigon, J. (1994) ^{1}H NMR studies of the high-affinity Rev binding site of the Rev responsive element of HIV-1 messenger RNA: Base pairing in the core binding element, *Biochemistry 33*, 5357−5366.
25. Battiste, J. L., Tan, R. Y., Frankel, A. D., and Williamson, J. R. (1994) Binding of an HIV Rev peptide to Rev responsive element RNA induces formation of purine-purine base pairs, *Biochemistry 33*, 2741−2747.
26. Battiste, J. L., Tan, R. Y., Frankel, A. D., and Williamson, J. R. (1995) Assignment and modeling of the Rev response element RNA bound to a Rev peptide using ^{13}C heteronuclear NMR, *J. Biomol. NMR 6*, 375−389.
27. Gosser, Y., Hermann, T., Majumdar, A., Hu, W. D., Frederick, R., Jiang, F., Xu, W. J., and Patel, D. J. (2001) Peptide-triggered conformational switch in HIV-1 RRE RNA complexes, *Nat. Struct. Biol. 8*, 146−150.
28. Ippolito, J. A., and Steitz, T. A. (2000) The structure of the HIV-1 RRE high affinity Rev binding site at 1.6 Å resolution, *J. Mol. Biol. 295*, 711−717.
29. Daly, T. J., Rennert, P., Lynch, P., Barry, J. K., Dundas, M., Rusche, J. R., Doten, R. C., Auer, M., and Farrington, G. K. (1993) Perturbation of the carboxy terminus of HIV-1 Rev affects multimerization on the Rev responsive element, *Biochemistry 32*, 8945−8954.
30. Malim, M. H., and Cullen, B. R. (1991) HIV-1 structural gene expression requires the binding of multiple Rev monomers to the viral RRE: Implications for HIV-1 latency, *Cell 65*, 241−248.
31. Thomas, S. L., Oft, M., Jaksche, H., Casari, G., Heger, P., Dobrovnik, M., Bevec, D., and Hauber, J. (1998) Functional analysis of the human immunodeficiency virus type 1 Rev protein oligomerization interface, *J. Virol. 72*, 2935−2944.
32. Sharpe, S., Kessler, N., Anglister, J. A., Yau, W. M., and Tycko, R. (2004) Solid state NMR yields structural constraints on the V3 loop from HIV-1 gp120 bound to the 447-52d antibody Fv fragment, *J. Am. Chem. Soc. 126*, 4979−4990.
33. Weliky, D. P., Bennett, A. E., Zvi, A., Anglister, J., Steinbach, P. J., and Tycko, R. (1999) Solid state NMR evidence for an antibody-dependent conformation of the V3 loop of HIV-1 gp120, *Nat. Struct. Biol. 6*, 141−145.
34. Litovchick, A., and Rando, R. R. (2003) Stereospecificity of short Rev-derived peptide interactions with RRE IIB RNA, *RNA 9*, 937−948.
35. Pines, A., Gibby, M. G., and Waugh, J. S. (1973) Proton-enhanced NMR of dilute spins in solids, *J. Chem. Phys. 59*, 569−590.
36. Hediger, S., Meier, B. H., and Ernst, R. R. (1995) Adiabatic passage Hartmann-Hahn cross-polarization in NMR under magic-angle sample spinning, *Chem. Phys. Lett. 240*, 449−456.
37. Metz, G., Wu, X. L., and Smith, S. O. (1994) Ramped-amplitude cross-polarization in magic-angle spinning NMR, *J. Magn. Reson., Ser. A 110*, 219−227.
38. Bennett, A. E., Rienstra, C. M., Auger, M., Lakshmi, K. V., and Griffin, R. G. (1995) Heteronuclear decoupling in rotating solids, *J. Chem. Phys. 103*, 6951−6958.
39. Bennett, A. E., Rienstra, C. M., Griffiths, J. M., Zhen, W. G., Lansbury, P. T., and Griffin, R. G. (1998) Homonuclear radiof-requency-driven recoupling in rotating solids, *J. Chem. Phys. 108*, 9463−9479.
40. Gullion, T., and Vega, S. (1992) A simple magic-angle spinning NMR experiment for the dephasing of rotational echoes of dipolar coupled homonuclear spin pairs, *Chem. Phys. Lett. 194*, 423−428.
41. Nishimura, S., Biggs, S., Scales, P. J., Healy, T. W., Tsunematsu, K., and Tateyama, T. (1994) Molecular-scale structure of the cation-modified muscovite mica basal plane, *Langmuir 10*, 4554−4559.
42. Wishart, D. S., and Case, D. A. (2001) Use of chemical shifts in macromolecular structure determination, *Methods Enzymol. 338*, 3−34.
43. Luca, S., Filippov, D. V., van Boom, J. H., Oschkinat, H., de Groot, H. J. M., and Baldus, M. (2001) Secondary chemical shifts in immobilized peptides and proteins: A qualitative basis for structure refinement under magic-angle spinning, *J. Biomol. NMR 20*, 325−331.
44. Iwadate, M., Asakura, T., and Williamson, M. P. (1999) C_α and C_β carbon-13 chemical shifts in proteins from an empirical database, *J. Biomol. NMR 13*, 199−211.
45. Dedios, A. C., Pearson, J. G., and Oldfield, E. (1993) Secondary and tertiary structural effects on protein NMR chemical-shifts: An ab initio approach, *Science 260*, 1491−1496.
46. Balbach, J. J., Ishii, Y., Antzutkin, O. N., Leapman, R. D., Rizzo, N. W., Dyda, F., Reed, J., and Tycko, R. (2000) Amyloid fibril formation by $A\beta_{16-22}$, a seven-residue fragment of the Alzheimer's β-amyloid peptide, and structural characterization by solid state NMR, *Biochemistry 39*, 13748−13759.
47. Spera, S., and Bax, A. (1991) Empirical correlation between protein backbone conformation and C_α and C_β ^{13}C nuclear magnetic resonance chemical shifts, *J. Am. Chem. Soc. 113*, 5490−5492.
48. Wishart, D. S., Sykes, B. D., and Richards, F. M. (1991) Relationship between nuclear magnetic resonance chemical shift and protein secondary structure, *J. Mol. Biol. 222*, 311−333.
49. Rout, M. P., Aitchison, J. D., Magnasco, M. O., and Chait, B. T. (2003) Virtual gating and nuclear transport: The hole picture, *Trends Cell Biol. 13*, 622−628.
50. Wishart, D. S., Bigam, C. G., Holm, A., Hodges, R. S., and Sykes, B. D. (1995) ^{1}H, ^{13}C and ^{15}N random coil NMR chemical shifts of the common amino-acids. 1. Investigations of nearest-neighbor effects, *J. Biomol. NMR 5*, 67−81.

BI0622928